sciendo INTERNATIONAL JOURNAL ON SMART SENSING AND INTELLIGENT SYSTEMS

Research Article | DOI: 10.2478/ijssis-2025-0057 Issue 1 | Vol. 18 (2025)

Enhancement of radial distribution network based on optimal location and sizing of photoVoltaic distributed generation using mountain gazelle optimizer and eel and grouper optimizer

Ghassan Abdullah Salman[1,2,*] and Layth Tawfeeq Al-Bahrani[1]

[1]Department of Electrical Engineering, College of Engineering, Mustansiriyah University, Baghdad, Iraq

[2]Department of Electrical Power and Machines, College of Engineering, University of Diyala, Diyala, Iraq

*E-mail: ghassanabdullah@uomustansiriyah.edu.iq; ghassanabdullah@uodiyala.edu.iq

Received for publication June 12, 2025.

Abstract

Due to the growth of loads in distribution networks and the increase in demand for electrical energy, providing energy from traditional sources has become a cause of huge losses, high costs, and environmental pollution. To avoid these problems, clean energy sources are the desired way to solve these problems by integrating Photovoltaic Distribution Generators (PVDG) into Radial Distribution Networks (RDN). Furthermore, detecting the optimal locations and sizes of PVDG is determined by modern approaches of optimization algorithms such as Mountain Gazelle Optimizer (MGO) and Eel and Grouper Optimizer (EGO). The proposed algorithms are applied to Multi-Objective Functions (MOF), including technical objective functions (OFs) and economic OF. Active Power Loss Index (APLI), Reactive Power Loss Index (RPLI), Voltage Deviation Index (VDI), and Voltage Stability Index (VSI) are the technical OFs, while the investment cost of PVDG (ICDG) is the economic OF. The efficiency and effectiveness of the proposed approaches are crucial and are achieved by the implemention of the standard test system (IEEE 69 bus), in addition to the Iraqi RDN (Iraqi 77 bus). Moreover, the simulation results carried out by the proposed algorithms have been verified for accuracy and validity compared with the results of previous articles. The overall performance of the networks is improved after incorporating the optimal allocations of PVDG in RDN; the voltage profile level and VSI are maximized for all buses, while the active and reactive power losses are minimized for all lines. On the other hand, the simulation results showed the dominance of the EGO technique over the MGO technique according to the speed and smoothness of convergence to the best solution with the minimum number of iterations.

Keywords

radial distribution networks, photovoltaic distribution generators, optimization algorithms (MGO and EGO), multi-objective functions, Iraqi radial networks

I. Introduction

Recently, attention has been directed toward clean energy to meet the increase in loads in the distribution system networks, because it is not harmful to the environment and reduces global warming. In addition to the environmental benefit, renewable energy sources provide technical benefits, such as reducing active and reactive power losses, improving voltage profile level and stability, and increasing reliability and resilience of the system networks. Renewable energy also provides an economic benefit by reducing operating and fuel costs, thus the economic benefit is reflected in favor of consumers [1–5]. Distribution generators are part of renewable energy sources; they can be defined as small units that are directly connected to the distribution network precisely at locations near to the load centers to ensure reliable power access for consumers. The integration of distribution generators in the distribution network leads to the flow of power in multiple directions instead of one direction. This technique is considered one of the benefits of distribution generators to improve the performance of the distribution network. Distribution generators must be controlled and not penetrate the distribution network largely and randomly, which would harm distribution networks [6–9].

According to the previous analysis of renewable energy sources, specifically distribution generator units, it is very important to detect the optimal locations and sizes of distribution generators to obtain the best performance of the distribution network. Many research papers and researchers have addressed the dilemma of finding optimization strategies to improve the performance of radial distribution networks (RDN), and the analytical methods have been proposed by a group of researchers to find solutions to the problems of optimal locations and sizes of distribution generators [10–12]. On the other hand, in [13–15] many optimization algorithms have been used to find the solutions of optimal locations and sizes of distribution generators.

In this paper, the results are compared with previous literature to find the optimal locations and sizes. In Sultana & Roy [16], the multi-objective semi-opposite teaching-based learning optimization was proposed to improve technical objectives (power loss reduction, voltage stability index [VSI], and voltage deviation) of an RDN. In Nagaballi & Kale [17], the Jaya algorithm, which is a modified teaching-learning-based optimization, the gray wolf optimizer was introduced to find a set of best solutions between technical and economic objectives. In Sharma et al. [18], the quasi-oppositional swine influenza model-based optimization with quarantine algorithm has been presented to reduce power losses in the network, improve voltage regulation, and improve voltage stability within system operation and safety constraints in RDN. In Imran et al. [19], the fireworks algorithm was proposed to reconfigure and allocate optimal distributed power generation units in the distribution network simultaneously, with the aim of reducing power loss and enhancing voltage stability. In Rao et al. [20], the harmony search algorithm was presented to solve the problem of network reconfiguration in the presence of distributed generation (DG) to minimize real power losses and improve the voltage profile in the distribution system. In Kowsalya [21], the bacterial foraging optimization was proposed to reduce grid power losses, minimize operating costs, and improve voltage stability. In Balu & Mukherjee [22], the Harris hawks optimization technique was provided to reduce active power loss (APL), total voltage deviation, and VSI of RDN. In Khasanov et al. [23], the Henry gas solubility optimization method was presented to reduce total power losses. Standard 33 bus and 69 bus test systems were used to verify the effectiveness of the proposed method. In Uniyal & Sarangi [24], the adaptive modified whale optimization algorithm was proposed to improve the voltage stability and loss profile of the distribution system, taking into account the probabilistic loads and DGs operating at varying power factors. In El-Maksoud et al. [25], the modified particle swarm optimization was proposed to simultaneously optimize distribution network reconfiguration and allocation of multiple DG units to minimize the total real power loss of the RDN.

Referring to the related literature of the above presentation of the previous literature in this paper, the essential contributions can be summarized as follows:

- Proposing modern approaches of optimization techniques such as mountain gazelle optimizer (MGO) and Eel and grouper optimizer (EGO) to detect the PVDG location and size in RDN.
- Improving technical and economic aspects of RDN is satisfied using PVDG based on the proposed algorithms.
- Applying the proposed algorithms with a single objective function (OF) (active power loss index [APLI] and VSI) and multiple objective functions (MOF).
- Implementing the proposed algorithms on the standard RDN such as IEEE 69 BUS.

- Implementing the proposed algorithms on the practical RDN such as IRAQI 77 BUS.
- Finally, comparing and analyzing previous studies to assess the effectiveness of the proposed algorithms.

This paper is presented as follows: section (Introduction) provides the literature survey of the previous papers and the main contribution of this paper, section (Problem formulation) presents the mathematical model of RDN and PVDG as OF with constraints, section (Optimization algorithms) describes the behaviors of MGO and EGO techniques for detecting the optimal location and sizing of PVDG in RDN, section (Study and simulation results) presents and discusses the numerical results and compares them with previous results, and section (Conclusion) provides the conclusion and future work of this paper.

II. Problem Formulation

In this part of the paper, the goal is to minimize a Multi-Objective Function (MOF) using a Photovoltaic Distribution Generator (PVDG). MOF is represented by the APLI, the Reactive Power Loss Index (RPLI), the Voltage Deviation Index (VDI), the VSI, and the Investment Cost of PVDG units (ICDG).

a. APLI

The first OF_1 is obtained by minimizing APLI; this OF has been adopted in Refs [26–28], which is expressed mathematically by the following equations:

$$\mathrm{OF}_1 = \min\left(\mathrm{APLI}\right)\ldots \tag{1}$$

$$\mathrm{APLI} = \frac{\mathrm{APL}^{\mathrm{WithDG}}}{\mathrm{APL}^{\mathrm{WithoutDG}} + \mathrm{APL}^{\mathrm{WithDG}}}\ldots \tag{2}$$

$$\mathrm{APL} = \sum_{\substack{i=1 \\ j\neq i, j>i}}^{N_B}\sum_{j=2}^{N_B}\left(\frac{\left|V_i - V_j\right|}{\left|R_{ij} + X_{ij}\right|}\right)^2 \times R_{ij}\ldots \tag{3}$$

where APL is the active power loss, N_B is the buses' number in RDN, V_i is the voltage at i^{th} bus, V_j is the voltage at j^{th} bus, R_{ij} is the resistance between buses i^{th} and j^{th}, and X_{ij} is the reactance between buses i^{th} and j^{th}.

b. RPLI

The second OF_2 is obtained by minimizing RPLI; this OF has been adopted in Refs [28, 29], which is expressed mathematically by the following equations:

$$OF_2 = \min\left(\mathrm{RPLI}\right)\ldots \tag{4}$$

$$\mathrm{RPLI} = \frac{\mathrm{RPL}^{\mathrm{WithDG}}}{\mathrm{RPL}^{\mathrm{WithoutDG}} + \mathrm{RPL}^{\mathrm{WithDG}}}\ldots \tag{5}$$

$$\mathrm{RPL} = \sum_{\substack{i=1 \\ j\neq i, j>i}}^{N_B}\sum_{j=2}^{N_B}\left(\frac{\left|V_i - V_j\right|}{\left|R_{ij} + X_{ij}\right|}\right)^2 * X_{ij}\ldots \tag{6}$$

where, RPL is the reactive power loss, N_B is the buses' number of RDN, V_i is the voltage at i^{th} bus, V_j is the voltage at j^{th} bus, R_{ij} is the resistance between buses i^{th} and j^{th}, and X_{ij} is the reactance between buses i^{th} and j^{th}.

c. VDI

The third OF_3 is obtained by minimizing VDI; this OF has been adopted in Refs [28, 30], which is expressed mathematically by the following equations:

$$\mathrm{OF}_3 = \min\left(\mathrm{VDI}\right)\ldots \tag{7}$$

$$\mathrm{VDI} = \left|\frac{\sum_{i=1}^{N_B} V_i}{N_B} - 1\right|\ldots \tag{8}$$

where, N_B is the buses' number of RDN, V_i is the voltage at i^{th} bus.

d. VSI

The fourth OF_4 is obtained by minimizing the inverse of the VSI; the limit of VSI lies between [1 0], where 1 refers to the best value while 0 refers to the collapse point; this OF has been adopted in Refs [30–32], which is expressed mathematically by the following equations:

$$OF_4 = \min\left(\frac{1}{\mathrm{VSI}}\right)\ldots \tag{9}$$

$$\mathrm{VSI} = \frac{1}{N_B}\sum_{\substack{i=1 \\ j\neq i, j>i}}^{N_B}\sum_{j=2}^{N_B}\left[\left|V_i\right|^4 - 4\left(P_j R_{ij} - Q_j X_{ij}\right)^2 - 4\left(P_j X_{ij} - Q_j R_{ij}\right)^2 * \left|V_i\right|^2\right]\ldots \tag{10}$$

where, N_B is the buses' number of RDN, V_i is the voltage at i^{th} bus, P_j is the active power at j^{th} bus, Q_j is the

reactive power at j^{th} bus, R_{ij} is the resistance between buses i^{th} and j^{th}, and X_{ij} is the reactance between buses i^{th} and j^{th}.

e. Investment Cost of PVDG (ICDG)

The fifth OF_5 is obtained by minimizing ICDG; this OF has been adopted in Refs [33, 34], which is expressed mathematically by the following equations:

$$OF_5 = \min\left(\text{ICDG}\right)\ldots \tag{11}$$

$$\text{ICDG} = \frac{1}{S_B}\sum_{i=1}^{N_{\text{DG}}} C_{\text{DG},i} * P_{\text{DG},i}\ldots \tag{12}$$

$$C_{\text{DG}} = C_{\text{Capital}} + C_{O\text{ and }M}\ldots \tag{13}$$

where, S_B is the base MVA, N_{DG} is the number of PVDG installed in RDN, $C_{\text{DG},i}$ is the cost of PVDG at i^{th} bus, $P_{\text{DG},i}$ is the active power of PVDG at i^{th} bus, C_{Capital} is the capital cost of PVDG, $C_{O\text{ and }M}$ is the operation and maintenance cost of PVDG.

MOF represents the sum of the OFs that have been stated individually and can be represented mathematically by the following equation:

$$\text{MOF} = \frac{1}{N_{\text{OF}}}\left(\text{OF}_1 + \text{OF}_2 + \text{OF}_3 + \text{OF}_4 + \text{OF}_5\right)\ldots \tag{14}$$

where, N_{OF} is the number of OFs and equal to 5 in this paper.

f. Equality and inequality constraints

To implement MOF, a set of equality and inequality constraints must be satisfied, the active and reactive power balanced, such as equality constraints, which are expressed mathematically by the following equations:

$$P_{\text{slack}} + \sum_{i=1}^{N_{\text{DG}}} P_{\text{DG},i} = \sum_{i=1}^{N_B} P_i^D + \text{APL}\ldots \tag{15}$$

$$Q_{\text{slack}} = \sum_{i=1}^{N_B} Q_i^D + \text{RPL}\ldots \tag{16}$$

where, P_{slack} is the active power generation from slack bus (bus 1), Q_{slack} is the reactive power generation from slack bus (bus 1), N_{DG} is the number of PVDG installed in RDN, $P_{\text{DG},i}$ is the active power of PVDG at i^{th} bus, N_B is the buses number of RDN, P_i^D is the total active power demand of RDN, Q_i^D is the total reactive power demand of RDN.

The voltage limits and PVDG unit limits, such as inequality constraints, are expressed mathematically by the following equations:

$$V_i^{\min} \le V_i \le V_i^{\max}\ldots \tag{17}$$

$$P_{\text{DG},i}^{\min} \le P_{\text{DG},i} \le P_{\text{DG},i}^{\max}\ldots \tag{18}$$

$$\sum_{i=1}^{N_{\text{DG}}} P_{\text{DG},i} \le \sum_{i=1}^{N_B} P_i^D + \text{APL}\ldots \tag{19}$$

$$2 \le \text{DG}_{\text{Location}} \le N_B\ldots \tag{20}$$

where, V_i is the voltage at i^{th} bus, $V_i^{\min}$ is the minimum voltage at i^{th} bus, $V_i^{\max}$ is the maximum voltage at i^{th} bus, $P_{DG,i}$ is the active power of PVDG at i^{th} bus, $P_{\text{DG},i}^{\min}$ is the minimum active power of PVDG at i^{th} bus, $P_{\text{DG},i}^{\max}$ is the maximum active power of PVDG at i^{th} bus, N_{DG} is the number of PVDG installed in RDN, N_B is the buses number of RDN, P_i^D is the total active power demand of RDN, $\text{DG}_{\text{Location}}$ is the location of PVDG in RDN.

III. Optimization Algorithms

In this part of the paper, two modern approaches of optimization algorithms have been proposed to detect optimal location and sizing of PVDG in RDN. These optimization algorithms are MGO and EGO. The optimization algorithms are generally implemented in Figure 1. In this figure, each algorithm is explained separately and represented by the red rectangle line (or box).

a. MGO

The MGO is a modern optimization technique that depends on the search for food during the migration of gazelle herds. Mountain gazelles consist of three groups: adult male gazelle herds (territorial), young male gazelle herds, and female gazelle herds with offspring. During the optimization process, any gazelle can be a member of any group [35, 36]. The MGO can be represented mathematically using the following stages:

While modeling Territorial Solitary Males (TSM), young gazelle males try to dominate the female gazelles' territories, and as strong adult male gazelles maintain and protect these territories, this stage is expressed by the following equation:

$$\text{TSM} = \text{male}_{\text{gazelle}} - \left|\left(ri_1 \times \text{BH} - ri_2 \times X\left(\text{iter}\right) \times F\right)\right| \times \text{Cof}_i\ldots \tag{21}$$

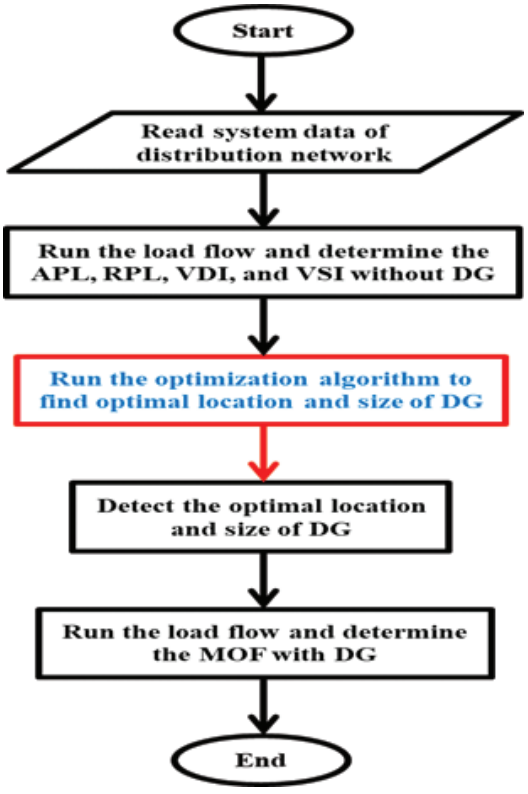

Figure 1: Flowchart of the proposed optimization algorithms. APL, active power loss; DG, distributed generation; RPL, reactive power loss; VDI, voltage deviation index; VSI, voltage stability index.

where, $\text{male}_{\text{gazelle}}$ is the location vector of the best adult gazelle male, ri_1 and ri_2 are random coefficient numbers either be 1 or 2, X(iter) is the location of young gazelle males at current iteration, BH is the effect factor of young gazelle male herds and is computed by Eq. (22), F is a factor based on iteration and compute by Eq. (23), Cof_i is a coefficient vector use to improve search ability and is computed by Eq. (24).

$$\text{BH} = X_{\text{ra}} * \lfloor r_1 \rfloor + M_{\text{pr}} \times \lceil r_2 \rceil, \text{ra} = \left\{ \frac{N}{3} \ldots N \right\} \ldots \quad (22)$$

where X_{ra} represents a random solution of young gazelle males, ra is the interval of young gazelle males, M_{pr} is the average value selected randomly for search agents, r_1 and r_2 are random coefficient numbers that lie between 0 and 1, N is the number of population.

$$F = N_1(D) \times \exp^{\left(2 - \text{iter} \times \left(\frac{2}{\text{maxiter}}\right)\right)} \ldots \quad (23)$$

$$\text{Cof}_i = \begin{cases} (a+1) + r_3, \\ a * N_2(D), \\ r_4(D), \\ N_3(D) * N_4(D)^2 * \cos\left((r_4 * 2) * N_3(D)\right) \end{cases} \ldots \quad (24)$$

where N_1, N_2, N_3, and N_4 are random numbers of standard distribution within problem dimensions, r_3 and r_4 are random coefficient numbers that lie between 0 and 1, a represents control coefficient that lies between –2, –1 and compute by Eq. (25).

$$a = -1 + \text{iter} \times \left(\frac{-1}{\text{maxiter}}\right) \ldots \quad (25)$$

Modeling Maternity Herds (MH)— while adult male gazelles age and lose their strength, young male gazelles attempt to dominate the female gazelle herds' territories to mate with females and produce new offspring, and this stage is expressed by the following equation:

$$\text{MH} = \left(\text{BH} + \text{Cof}_{1,i}\right) + \left(ri_3 \times \text{male}_{\text{gazelle}} - ri_4 \times X_{\text{rand}}\right) \times \text{Cof}_{2,i} \ldots \quad (26)$$

where BH is the effect factor of young gazelle male herds and is computed by Eq. (22), $\text{Cof}_{1,i}$ and $\text{Cof}_{2,i}$ are coefficient vectors used to improve search ability and are computed by Eq. (24), $\text{male}_{\text{gazelle}}$ is the location vector of the best adult gazelle male, ri_3 and ri_3 are random coefficient numbers either be 1 or 2, X_{rand} is the location vector of random gazelle.

Modeling Bachelor Male Herds (BMH)— after the young male gazelles complete their growth and reach adulthood, they try to create new territories and dominate female gazelles. Consequently, violent conflicts occur between them and older males. The following equation expresses this stage:

$$\text{BMH} = \left(X(\text{iter}) - D\right) + \left(ri_5 \times \text{male}_{\text{gazelle}} - ri_6 \times \text{BH}\right) \times \text{Cof}_i \ldots \quad (27)$$

where X(iter) is the location of young gazelle males at current iteration, $\text{male}_{\text{gazelle}}$ is the location vector of the best adult gazelle male, BH is the effect factor of young gazelle male herds and is computed by Eq. (22), Cof_i is a coefficient vector used to improve search ability and is computed by Eq. (24), ri_5 and ri_6 are random coefficient numbers either be 1 or 2, D is the coefficient vector affected by best solution and current agents and is computed by Eq. (28).

$$D = \left(\left|X(\text{iter})\right| + \left|\text{male}_{\text{gazelle}}\right|\right) \times \left(2 \times r_5 - 1\right) \ldots \quad (28)$$

where X(iter) is the location of young gazelle males at the current iteration, $\text{male}_{\text{gazelle}}$ is the location vector of the best adult gazelle male, r_5 is a random coefficient number which lies between 0 and 1.

Modeling Migration in search of food (MSF)—mountain gazelles have the capability to run quickly and jump, which helps to move long distances and migrate in search of food sources and this stage is expressed by the following equation:

$$\text{MSF} = (ub - lb) * r_6 + lb \ldots \quad (29)$$

where ub and lb are the upper and lower limits of the OF, r_6 is random coefficient number that lies between 0 and 1.

A flow chart has been shown in Figure 2 for optimal location and sizing of PVDG in RDN using MGO.

b. EGO

The EGO is a modern optimization technique based on the principle of cooperative or symbiotic participation between grouper fish and moray eel to hunt

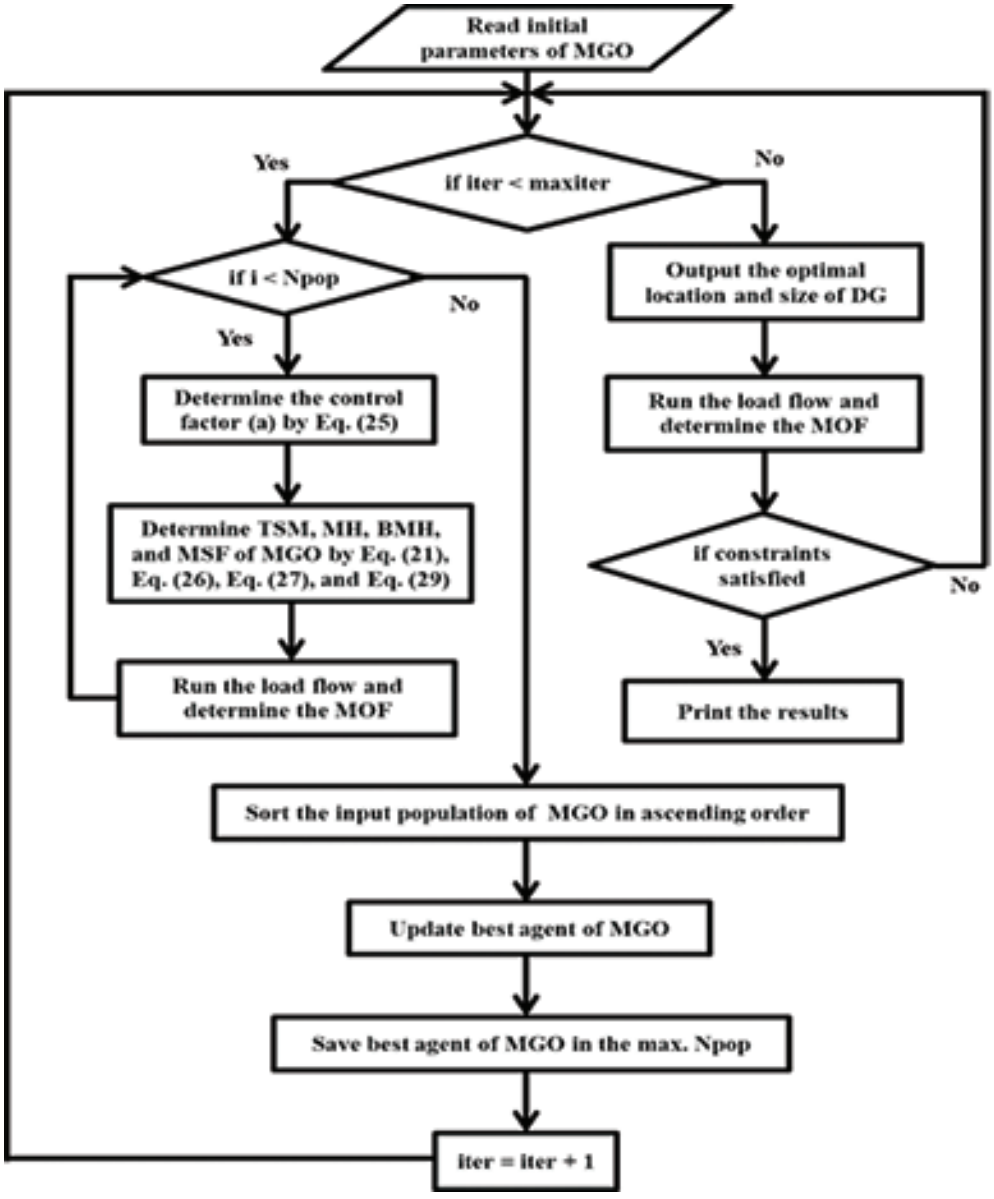

Figure 2: Flowchart of the proposed MGO. BMH, bachelor male herds; DG, distributed generation; MH, maternity herds; MGO, mountain gazelle optimizer; MSF, migration to search of food; TSM, territorial solitary males.

prey and search for food. Grouper hunts prey in open water while eel have the ability to penetrate coral reefs. Consequently, grouper tracks prey and send signals to the eel to carry out the cooperative or symbiotic pursuit and hunting process [37, 38]. To implement the EGO mathematically, the following processes can be used.

The process of exploration is the process of tracking prey by the grouper; grouper seeks to find the best OF based on the location of the prey, while the eel location is chosen randomly that rests nearby close to location of the prey. This process is modeled by the following equations:

$$\vec{X}_i^{\text{iter}+1} = \vec{X}_{\text{rand}} + \vec{C_1} \times \left| \vec{X}_i^{\text{iter}} - \vec{C_2} \times \vec{X}_{\text{rand}} \right| \ldots \quad (30)$$

$$\overrightarrow{XG}_i^{\text{iter}+1} = \vec{X}_i^{\text{iter}+1},\ if\ \text{fitness}\left(\vec{X}_i^{\text{iter}+1}\right) > \overrightarrow{XG}_i^{\text{iter}} \ldots \quad (31)$$

$$\vec{C_1} = 2a \times r_1 - a \ldots \quad (32)$$

$$\vec{C_2} = 2r_2 \ldots \quad (33)$$

$$a = 2 - 2 \times \left(\frac{\text{iter}}{\text{maxiter}} \right) \ldots \quad (34)$$

$$r_3 = (a-2) \times r_1 + 2 \ldots \quad (35)$$

$$r_4 = 100 \times \text{rand} \ldots \quad (36)$$

where $\vec{X}_{\text{rand}}$ is the random location vector, $\vec{X}_i^{\text{iter}}$ and $\vec{X}_i^{\text{iter}+1}$ are the best solution in the i^{th} dimension at current iteration and at (*iter* + 1), $\overrightarrow{XG}_i^{\text{iter}}$ and $\overrightarrow{XG}_i^{\text{iter}+1}$ are the locations of grouper in the i^{th} dimension at current iteration and at (iter + 1), *rand*, r_1 and r_2 are random coefficient numbers that lies between 0 and 1, *a* is a shrinkage factor and reduced from 2 to 0, r_3 is random coefficient number lies between 0, *a*, r_4 is random coefficient number lies between 0 and 100, $\vec{C_1}$ is the coefficient vector that lies between –*a* and a, $\vec{C_2}$ is the coefficient that vector lies between 0 and 2.

The process of sending a signal from grouper to moray eel, after grouper's prey escapes to the coral reef, the grouper sends a signal to a nearby moray eel in the crevice by head shaking and moving its dorsal fin. This process is modeled by the following equations:

$$\overrightarrow{XE}_i^{\text{iter}} = \vec{C_2} * \overrightarrow{XG}_i^{\text{iter}},\ if\ r_4 \le \text{starvation\_rate} \ldots \quad (37)$$

$$\text{starvation\_rate} = 100 \times \left(\frac{\text{iter}}{\text{maxiter}} \right) \ldots \quad (38)$$

where r_4 is random coefficient number that lies between 0 and 100, $\vec{C_2}$ is the coefficient vector that lies between 0 and 2, starvation_rate is the coefficient number that lies between 0 and 100, $\overrightarrow{XG}_i^{\text{iter}}$ is the location of grouper in the i^{th} dimension at current iteration, and $\overrightarrow{XE}_i^{\text{iter}}$ is the location of eel in the i^{th} dimension at current iteration.

The process of exploitation (associative process) is the process of cooperative or symbiotic participation to attack prey, and in this process, the chances of catching prey increase and this process is modeled by the following equations:

$$X_1 = e^{br_3} \times \sin(2\pi r_3) \times \vec{C_1} \left| \overrightarrow{XE}_i^{\text{iter}} - \overrightarrow{XP}_i^{\text{iter}} \right| + \overrightarrow{XE}_i^{\text{iter}},\ b = a \times r_2 \ldots \quad (39)$$

$$X_2 = \overrightarrow{XG}_i^{\text{iter}} + \vec{C_1} \times \left| \overrightarrow{XG}_i^{\text{iter}} - \overrightarrow{XP}_i^{\text{iter}} \right| \ldots \quad (40)$$

$$\vec{X}_i^{\text{iter}+1} = \begin{cases} \dfrac{0.8X_1 + 0.2X_2}{2}, if\ p < 0.5 \\ \dfrac{0.2X_1 + 0.8X_2}{2}, if\ p \ge 0.5 \end{cases} \ldots \quad (41)$$

where *a* is a shrinkage factor and reduced from 2 to 0, r_3 is random coefficient number that lies between 0 and *a*, $\vec{C_1}$ is the coefficient vector that lies between –*a* and *a*, $\overrightarrow{XG}_i^{\text{iter}}$ is the location of grouper in the i^{th} dimension at current iteration, $\overrightarrow{XE}_i^{\text{iter}}$ is the location of eel in the i^{th} dimension at current iteration, $\overrightarrow{XP}_i^{\text{iter}}$ is the location of prey in the i^{th} dimension at current iteration, X_1 is the location of eel, X_2 is the location of grouper, *p* is a random coefficient number that lies between 0 and 1, and $\vec{X}_i^{\text{iter}+1}$ is the best solution in the i^{th} dimension at (iter + 1).

A flow chart has been represented in Figure 3 for optimal location and sizing of PVDG in RDN using EGO.

IV. Study and Simulation Results

In this paper, the proposed optimization algorithms have been implemented on the standard test of RDN such as IEEE 69 BUS and on the practical RDN of the Iraqi distribution grid, which is BAQ-CENTER-ALTABO-SARYA 77 BUS.

a. Standard: IEEE 69 BUSES

IEEE 69 BUS, as shown in Figure 4, consists of 68 lines, with a base voltage of 12.66 kV and a base MVA of 100 MVA. Bus 1 or Node 1 (green node) is the slack bus, the red nodes are load buses, and the blue

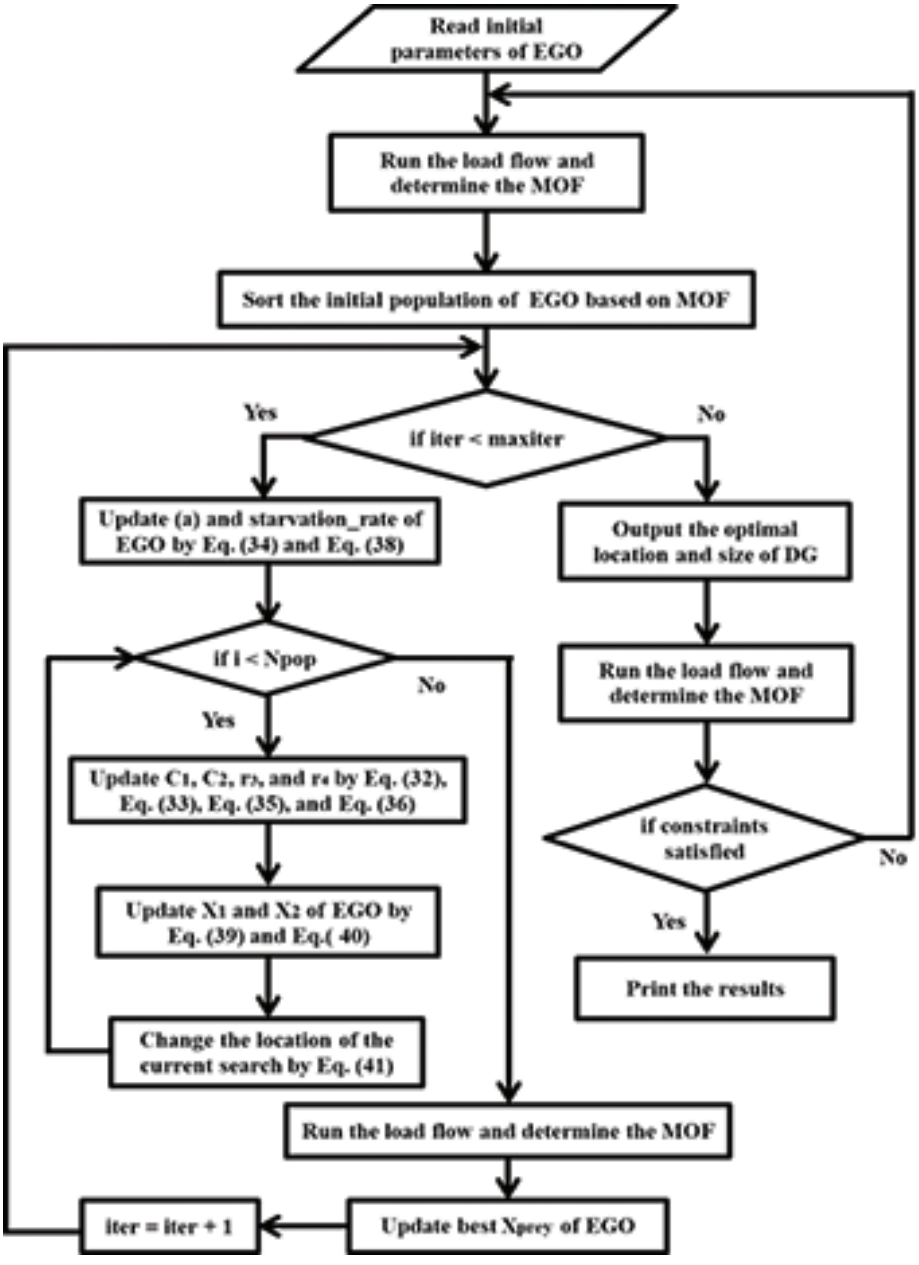

Figure 3: Flowchart of the proposed EGO. DG, distributed generation; EGO, Eel and grouper optimizer.

nodes are connection buses (load buses but not connected to distribution transformers); the total active power load is 3802 kW while the total reactive power load is 2694 kVAR [39]. The total APL is 224.96 kW, the total RPL is 102.14 kVAR, the VDI is 0.0266, and the VSI is 0.9017. These values represent the power flow results of the IEEE 69 BUS at the base case. To demonstrate the effectiveness of the proposed optimization algorithms carried out in two cases as a single OF and compared with previous papers, the third case is applied on multi OFs using proposed optimization algorithms.

a.i. CASE1: Single OF (APL)

To detect the optimal location and capacity of PVDGs with APL as a single OF, the simulation results of optimization algorithms (MGO and EGO) provided in Table 1. observed that the APL is minimized from 224.96 kW to (71.19 and 71.00) kW for optimization

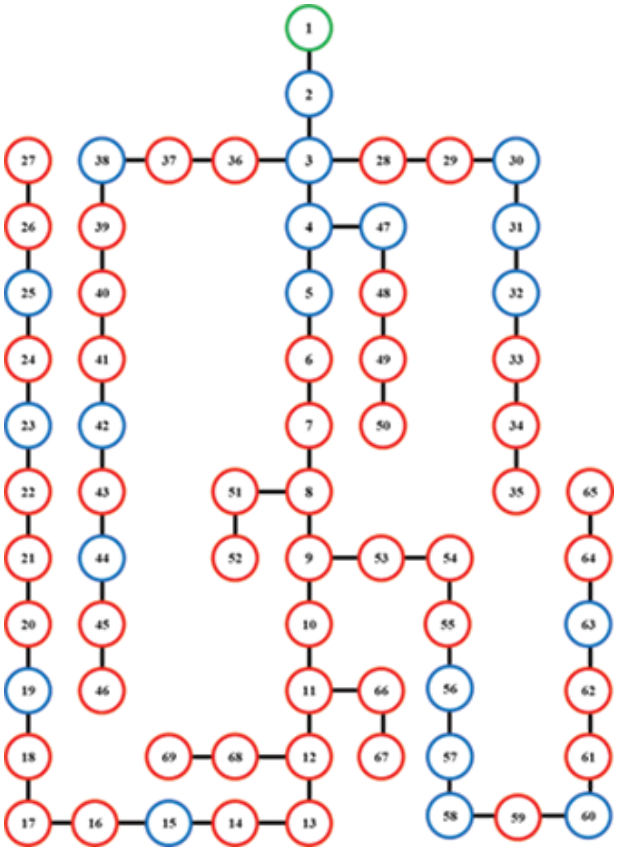

Figure 4: One-line diagram of IEEE 69 BUSES.

Table 1: Results of PVDG with minimized APL (IEEE 69 BUS)

	MGO	EGO
DG location	16, 61, 64	9, 18, 61
DG size (kW)	549.6, 1,482.7, 278.3	841.6, 449.3, 1,498.4
APL (kW)	71.19	71.00

APL, active power loss; DG, distributed generation; EGO, Eel and grouper optimizer; MGO, mountain gazelle optimizer.

techniques (MGO and EGO), respectively. The EGO has the best result compared with MGO, and also from the convergence behavior shown in Figure 5, it is observed that EGO converges to the best solution (minimum APL) compared with MGO. While Figure 6 shows the boxplot for the proposed techniques, the superiority of the EGO technique is demonstrated over the MGO technique.

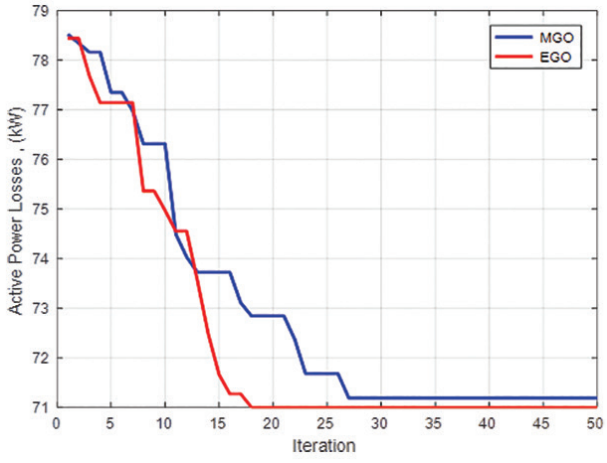

Figure 5: The convergence curve of APL (IEEE 69 BUS). APL, active power loss; EGO, Eel and grouper optimizer; MGO, mountain gazelle optimizer.

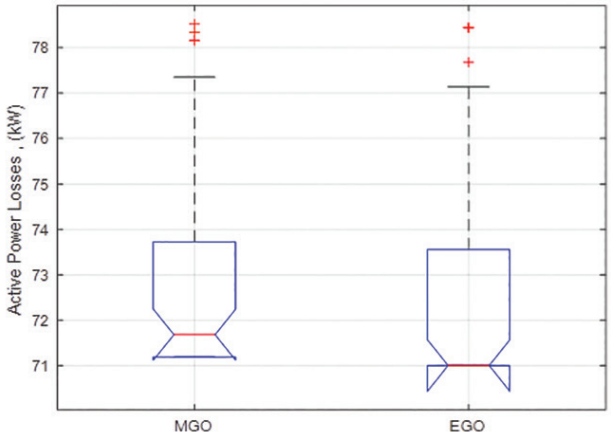

Figure 6: The boxplot of APL (IEEE 69 BUS). APL, active power loss; EGO, Eel and grouper optimizer; MGO, mountain gazelle optimizer.

On the other hand, the overall performances of RDN are enhanced when minimized by APL, where it is observed that the voltage profile is improved as shown in Figure 7, and all the buses' voltages have become more the minimum voltage limit (0.95 V) after incorporating PVDG. In addition, to demonstrate the effectiveness of the proposed algorithms, the results are compared with the results of previous papers, as given in Table 2.

a.ii. CASE2: Single OF (VSI)

The simulation results of optimization algorithms (MGO and EGO) to find the optimal placement and

size of PVDG with VSI as a single OF are given in Table 3; while the value of VSI is 0.9017 at base case, this value is maximized by using optimization techniques (MGO and EGO) to (0.9921 and 0.9947) respectively, and the value of VSI for EGO is better than the value of VSI for MGO. Figure 8 shows the convergence characteristics of optimization algorithms and is observed that EGO is close to best solution (maximum VSI) compared with MGO. While Figure 9 illustrates the boxplot for the proposed techniques, in which the superiority of EGO technique is demonstrated over MGO technique.

On the other hand, the overall performances of RDN are enhanced when maximized with VSI. It is observed that the voltage profile is enhanced as shown in Figure 10, and all the buses' voltages have

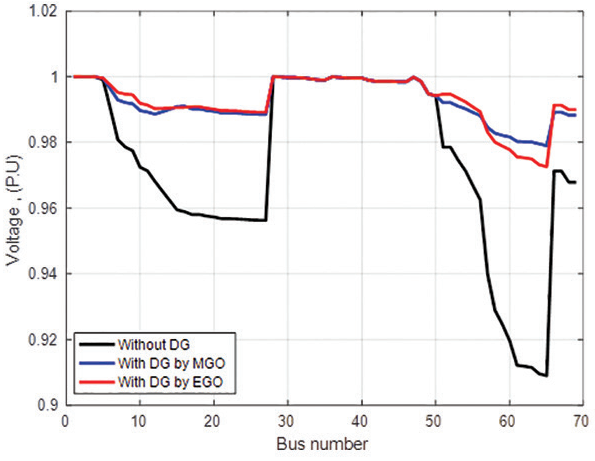

Figure 7: The voltage profile of case1 (IEEE 69 BUS). DG, distributed generation; EGO, Eel and grouper optimizer; MGO, mountain gazelle optimizer.

Table 3: Results of PVDG with maximized VSI (IEEE 69 BUS)

	MGO	EGO
DG location	26, 60, 64	23, 59, 61
DG size (kW)	1,032.8, 1,046.7, 1,083.4	1,306.3, 1,133.8, 1,084.5
VSI (P.U)	0.9921	0.9947
1/VSI (P.U)	1.0079	1.0053

DG, distributed generation; EGO, Eel and grouper optimizer; MGO, mountain gazelle optimizer; VSI, voltage stability index.

Table 2: Comparison results of PVDG with minimized APL (IEEE 69 BUS)

Method	DG location	DG size (kW)	APL (kW)
TLBO [16]	15, 61, 63	591.9, 818.8, 900.3	72.4
QTLBO [16]	18, 61, 63	533.4, 1,198.6, 567.2	71.6
JAYA [17]	12, 50, 61	1,016, 100, 2,000	75.83
MTLBO [17]	20, 57, 62	446, 477, 1,836	77.36
GWO [17]	12, 50, 61	792, 586, 2,000	73.43
SIMBO-Q [18]	17, 61, 67	428.5, 1,500, 486.3	71.4
QOSIMBO-Q [18]	9, 17, 61	831.4, 453.8, 1,500	71.0
FWA [19]	27, 61, 65	225.8, 1,198.6, 408.5	77.85
HSA [20]	63, 64, 65	1,302.4, 369, 101.8	86.77
BFOA [21]	27, 61, 65	295.4, 1,345.1, 447.6	75.23
HHO [22]	12, 61, 62	734.1, 1,191.2, 762.3	74.14
HGSO [23]	15, 57, 61	598.63, 200, 1,796.9	72.33
AMWOA [24]	11, 18, 64	602, 589, 145	71.41
MPSO [25]	17, 61, 64	531, 1,490, 290	71.1
Propose MGO	16, 61, 64	549.6, 1,482.7, 278.3	71.19
Propose EGO	9, 18, 61	841.6, 449.3, 1,498.4	71.0

APL, active power loss; DG, distributed generation; EGO, Eel and grouper optimizer; MGO, mountain gazelle optimizer.

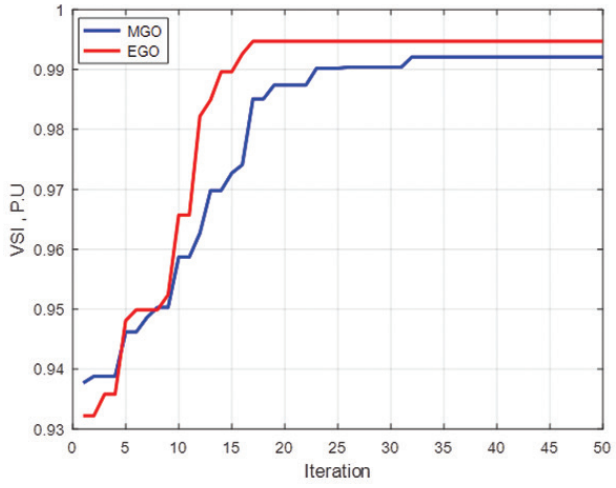

Figure 8: The convergence curve of VSI (IEEE 69 BUS). EGO, Eel and grouper optimizer; MGO, mountain gazelle optimizer; VSI, voltage stability index.

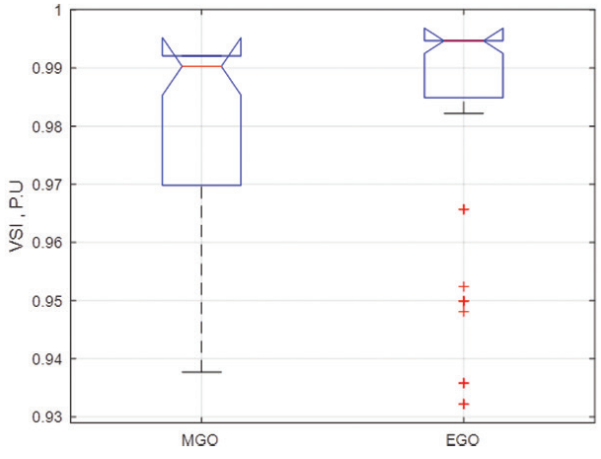

Figure 9: The boxplot of VSI (IEEE 69 BUS). VSI, voltage stability index.

become more than the minimum voltage limit (0.95 V) after inserting of PVDG. In addition, to demonstrate the effectiveness of the proposed algorithms, the results are compared with the results of previous papers, as given in Table 4.

a.iii. CASE3: Multi Objective Functions (MOF)

In this case, MOF, such as APLI, RPLI, VDI, the inverse of VSI, and investment Cost of PVDG (ICDG) are considered to obtain the optimal allocation (placement and capacity) of PVDG for RDN. Table 5 shows the result of these MOF on standard of IEEE 69 BUS based on both optimization techniques of MGO and EGO. It is clear that the overall performance of IEEE

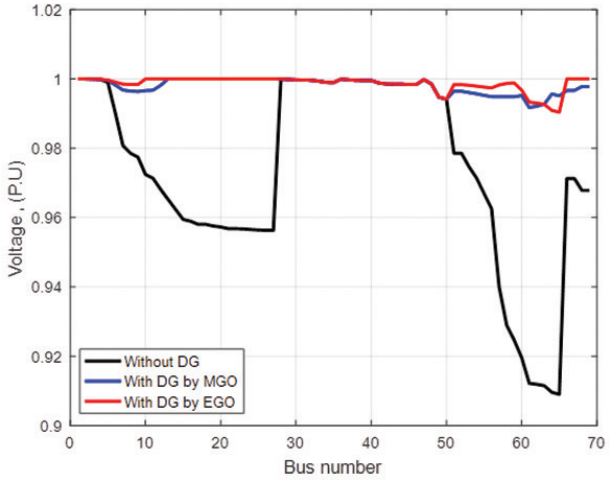

Figure 10: The voltage profile of case2 (IEEE 69 BUS). DG, distributed generation; EGO, Eel and grouper optimizer; MGO, mountain gazelle optimizer.

Table 4: Comparison results of PVDG with maximized VSI (IEEE 69 BUS)

Method	DG location	DG size (kW)	VSI (P.U)	1/VSI (P.U)
TLBO [16]	27, 60, 61	702.6, 1171.6, 1163	0.9762	1.0244
QTLBO [16]	22, 61, 62	1193.1, 1196.7, 1191.4	0.9770	1.0235
SIMBO-Q [18]	21, 63, 64	1384.1, 1500, 1055.5	0.9770	1.0235
QOSIMBO-Q [18]	12, 56, 63	1500, 1500, 1500	0.9771	1.0234
Propose MGO	26, 60, 64	1032.8, 1046.7, 1083.4	0.9921	1.0079
Propose EGO	23, 59, 61	1306.3, 1133.8, 1084.5	0.9947	1.0053

DG, distributed generation; EGO, Eel and grouper optimizer; MGO, mountain gazelle optimizer; VSI, voltage stability index.

Table 5: Results of PVDG with MOF (IEEE 69 BUS)

	MGO	EGO
DG location	24, 51, 62	17, 30, 61
DG size (kW)	455.1, 990.7, 1,608.6	580.5, 854.1, 1,742.3
APL (kW)	72.91	71.75
RPL (kVAR)	36.46	35.95
VDI (P.U)	0.0058	0.0071
VSI (P.U)	0.9770	0.9722
APLI (P.U)	0.2447	0.2418
RPLI (P.U)	0.2630	0.2603
ICDG ($)	0.1227	0.1207
MOF	0.3319	0.3316

APL, active power loss; APLI, active power loss index; DG, distributed generation; EGO, Eel and grouper optimizer; MGO, mountain gazelle optimizer; RPL, reactive power loss; RPLI, reactive power loss index; VDI, voltage deviation index; VSI, voltage stability index.

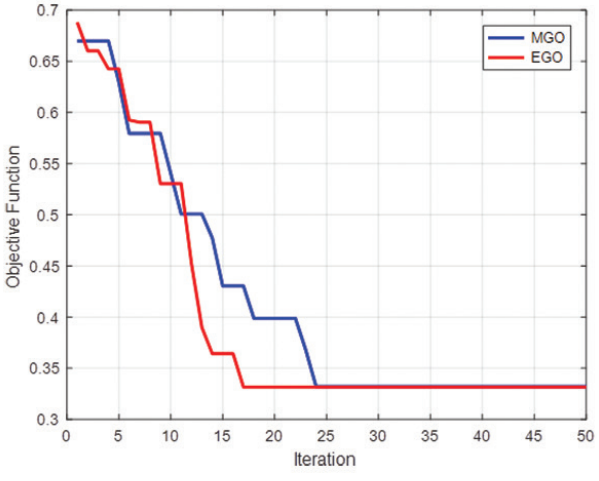

Figure 11: The convergence curve of MOF (IEEE 69 BUS). EGO, Eel and grouper optimizer; MGO, mountain gazelle optimizer.

69 BUS has been improved after integrating PVDG in the network. Both optimization algorithms (MGO and EGO) have shown their effectiveness and superiority compared to base case results. As well as the value of MOF using EGO leads to faster and smoother convergence compared with MGO as shown in Figure 11,

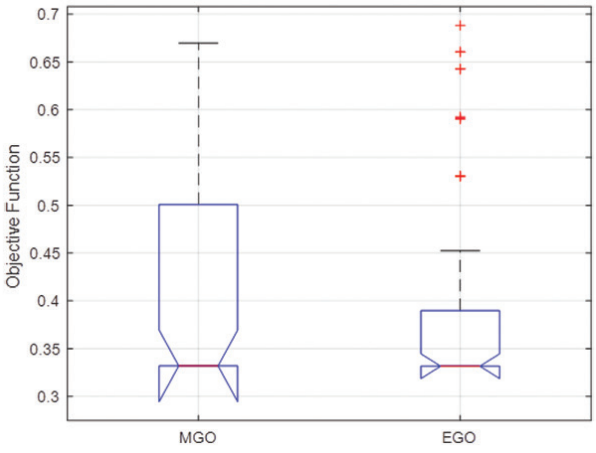

Figure 12: The boxplot of MOF (IEEE 69 BUS). EGO, Eel and grouper optimizer; MGO, mountain gazelle optimizer.

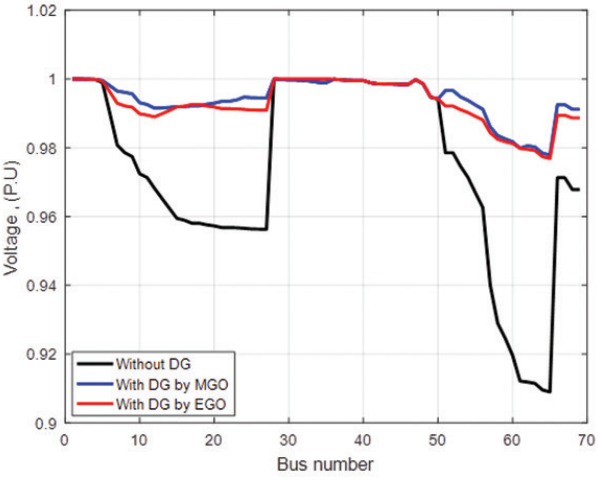

Figure 13: The voltage profile of case3 (IEEE 69 BUS). DG, distributed generation; EGO, Eel and grouper optimizer; MGO, mountain gazelle optimizer.

also Figure 12 exhibits the boxplot of the optimization techniques, and EGO technique is in dominance over MGO technique.

Moreover, to clarify the effectiveness of the proposed optimization techniques to determine the optimal allocation of PVDG on the performance of IEEE 69 BUS, the extent of enhancement in voltage profile is shown in Figure 13, while Figure 14 shows the extent of reduction in RPL.

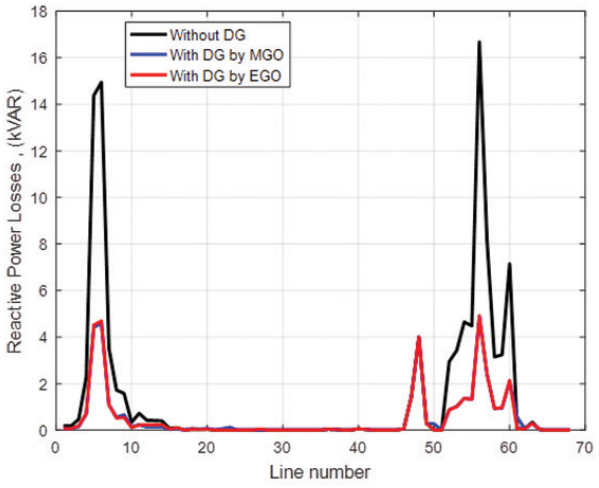

Figure 14: RPL of case3 (IEEE 69 BUS). DG, distributed generation; EGO, Eel and grouper optimizer; MGO, mountain gazelle optimizer; RPL, reactive power loss.

b. Practical: BAQ-CENTER-ALTABO-SARYA 77 BUSES

BAQ-CENTER-ALTABO-SARYA 77 BUS consists of 76 lines, the base voltage is 11 kV, the base MVA is 100 MVA. The one-line diagram is shown in Figure 15, node 1 (green node) is the slack bus, the red nodes are load buses, and the blue nodes are connection buses (load buses but not connected to distribution transformers); the total active power load is 21,426 kW while the total reactive power load is 13,259 kVAR. The total APL is 711.77 kW, the total RPL is 495.51 kVAR, the VDI is 0.0317, and the VSI is 0.8802. These values represent the power flow results of BAQ-CENTER-ALTABO-SARYA 77 BUS at base case. To prove the efficiency and effectiveness of the proposed techniques (MGO and EGO), the practical network of Iraqi 77 bus has been tested to obtain the optimal location and capacity of PVDG based on MOF and the results are given in Table 6. The system performance is clearly improved after adding PVDG.

Furthermore, when comparing the proposed algorithms, it is noted that EGO technique is superior to MGO technique, and it is noted that EGO technique converges to the optimal solution faster and with fewer iterations as shown in Figure 16, and the same in Figure 17 the boxplot shows precedence and dominance of EGO over MGO. Therefore, the behavior and performance of Iraqi 77 bus will improve

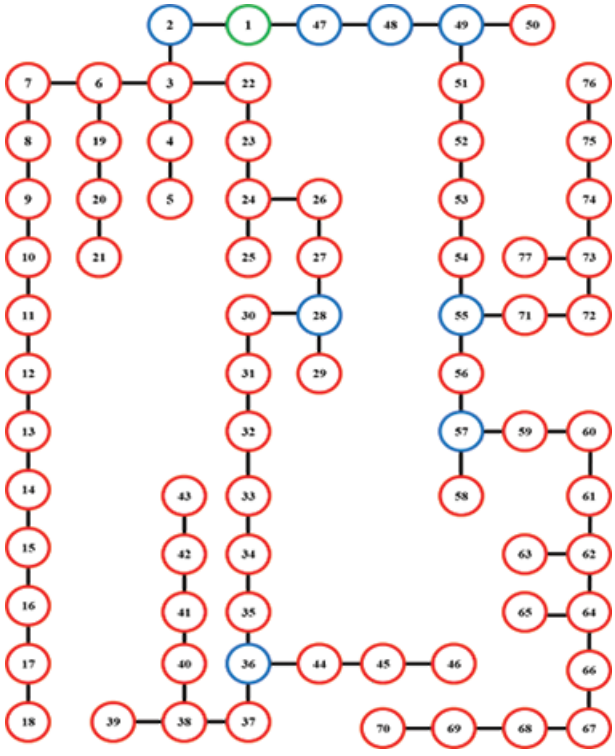

Figure 15: One-line diagram of IRAQI 77 BUSES.

Table 6: Results of PVDG with MOF (IRAQI 77 BUS)

	MGO	EGO
DG location	18, 41, 63	11, 40, 66
DG size (kW)	2,595.4, 2,796.3, 2,407.3	2,697.5, 2,860.7, 2,346.5
APL (kW)	367.75	361.41
RPL (kVAR)	257.75	253.45
VDI (P.U)	0.0214	0.0215
VSI (P.U)	0.9174	0.9172
APLI (P.U)	0.3406	0.3367
RPLI (P.U)	0.3421	0.3384
ICDG ($)	0.3135	0.3177
MOF	0.4215	0.4209

APL, active power loss; APLI, active power loss index; DG, distributed generation; EGO, Eel and grouper optimizer; MGO, mountain gazelle optimizer; RPL, reactive power loss; RPLI, reactive power loss index; VDI, voltage deviation index; VSI, voltage stability index.

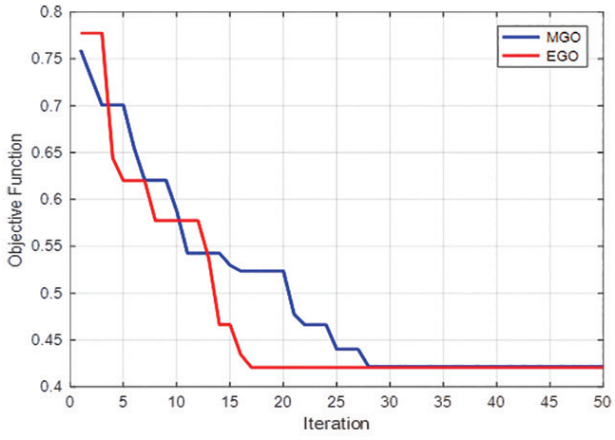

Figure 16: The convergence curve of MOF (IRAQI 77 BUS). EGO, Eel and grouper optimizer; MGO, mountain gazelle optimizer.

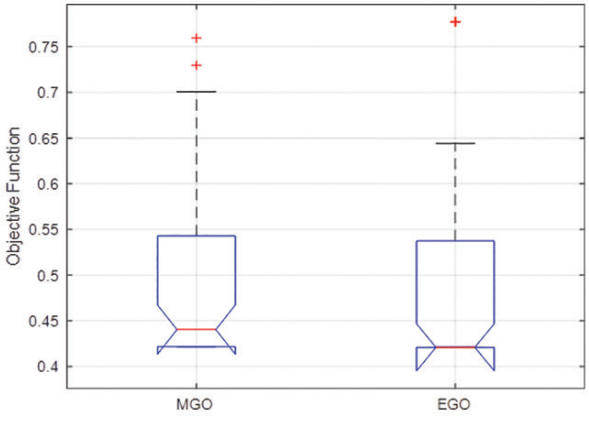

Figure 17: The boxplot of MOF (IRAQI 77 BUS). EGO, Eel and grouper optimizer; MGO, mountain gazelle optimizer.

after injecting PVDG, while the increasing level of voltage profile and VSI are introduced in Figure 18 and Figure 19 respectively; meanwhile, the reductions of APL and RPL are presented in Figure 20 and Figure 21, respectively.

V. Conclusion

Referring to the problems related to voltage deviation, voltage stability, power losses, and optimization allocation (siting and capacity) of Photovoltaic Distributed Generation (PVDG) in distribution system, this article proposes a modern approach of optimization techniques to solve these problems.

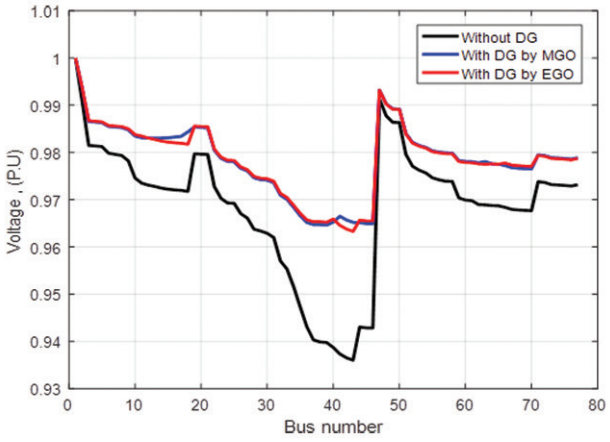

Figure 18: The voltage profile of MOF (IRAQI 77 BUS). DG, distributed generation; EGO, Eel and grouper optimizer; MGO, mountain gazelle optimizer.

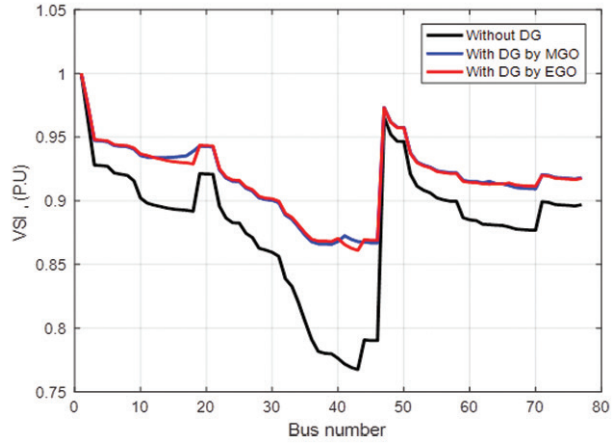

Figure 19: VSI of MOF (IRAQI 77 BUS). DG, distributed generation; EGO, Eel and grouper optimizer; MGO, mountain gazelle optimizer; VSI, voltage stability index.

The proposed optimization techniques are MGO and EGO. To demonstrate the effectiveness of these proposed optimization techniques and verify the accuracy of their results, a standard test system of IEEE 69 bus and a practical system of Iraqi 77 bus have been tested. The results showed the superiority of the proposed techniques compared to the techniques presented in previous literature. Furthermore, this article presented five OFs: APLI, RPLI, VDI, VSI, as the technical OFs, while the fifth OF is the Investment Cost of PVDG units (ICDG) as

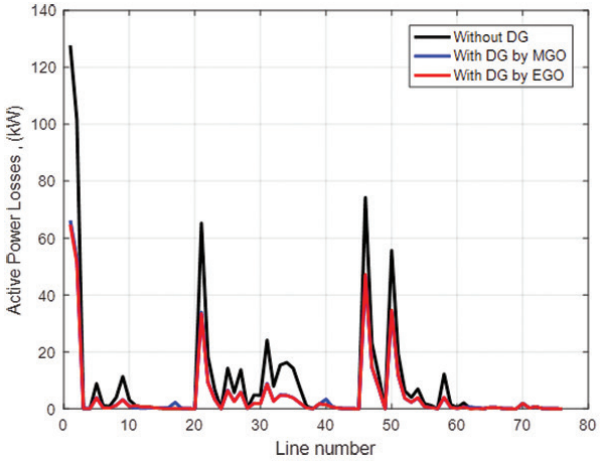

Figure 20: APL of MOF (IRAQI 77 BUS). APL, active power loss; DG, distributed generation; EGO, Eel and grouper optimizer; MGO, mountain gazelle optimizer.

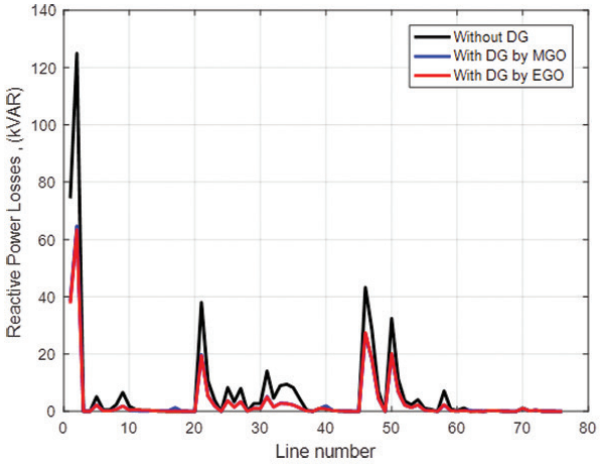

Figure 21: RPL of MOF (IRAQI 77 BUS). DG, distributed generation; EGO, Eel and grouper optimizer; MGO, mountain gazelle optimizer; RPL, reactive power loss.

the economical OF. The simulation results showed a significant improvement in the performance of both standard RDN and practical RDN after integrated PVDG in the networks. On the other hand, the comparison between the proposed algorithms led to determining the precedence and dominance of EGO technique over the MGO technique to reach the best solution in single and multi OF. This article can be highlighted in the future work by analyzing and studying the impact of PVDG on the resilience of RDN in the event of earthquakes, typhoons, or strong winds. Moreover, in the future, work can be utilized by the proposed algorithms to detect the optimal locations and sizes of FACTS devices such as Static VAR Compensator (SVC) and Thyristor Controlled Series Compensator (TCSC).

References

[1] Saber, A. Y., & Venayagamoorthy, G. K. (2010). Plug-in vehicles and renewable energy sources for cost and emission reductions. IEEE Transactions on Industrial electronics, 58(4), 1229-1238. DOI: 10.1109/TIE.2010.2047828

[2] Muttaqi, K. M., Le, A. D., Negnevitsky, M., & Ledwich, G. (2014). An algebraic approach for determination of DG parameters to support voltage profiles in radial distribution networks. IEEE Transactions on Smart Grid, 5(3), 1351-1360. DOI: 10.1109/TSG.2014.2303194

[3] Saha, S., & Mukherjee, V. (2016). Optimal placement and sizing of DGs in RDS using chaos embedded SOS algorithm. IET Generation, Transmission & Distribution, 10(14), 3671-3680. DOI: 10.1049/iet-gtd.2016.0151

[4] Ayalew, M., Khan, B., Giday, I., Mahela, O. P., Khosravy, M., Gupta, N., & Senjyu, T. (2022). Integration of renewable based distributed generation for distribution network expansion planning. Energies, 15(4), 1378. DOI: 10.3390/en15041378

[5] Stanelytė, D., & Radziukynas, V. (2022). Analysis of voltage and reactive power algorithms in low voltage networks. Energies, 15(5), 1843. DOI: 10.3390/en15051843

[6] Georgilakis, P. S., & Hatziargyriou, N. D. (2013). Optimal distributed generation placement in power distribution networks: models, methods, and future research. IEEE Transactions on power systems, 28(3), 3420-3428. DOI: 10.1109/TPWRS.2012.2237043

[7] Dorostkar-Ghamsari, M. R., Fotuhi-Firuzabad, M., Lehtonen, M., & Safdarian, A. (2015). Value of distribution network reconfiguration in presence of renewable energy resources. IEEE Transactions on Power Systems, 31(3), 1879-1888. DOI: 10.1109/TPWRS.2015.2457954

[8] Ali, A., Raisz, D., & Mahmoud, K. (2019). Optimal oversizing of utility-owned renewable DG inverter for voltage rise prevention in MV distribution systems. International Journal of Electrical Power & Energy Systems, 105, 500-513. DOI: 10.1016/j.ijepes.2018.08.040

[9] Ufa, R. A., Malkova, Y. Y., Rudnik, V. E., Andreev, M. V., & Borisov, V. A. (2022). A review on distributed generation impacts on electric power system. International journal of hydrogen energy, 47(47), 20347-20361. DOI: 10.1016/j.ijhydene.2022.04.142

[10] Viral, R., & Khatod, D. K. (2015). An analytical approach for sizing and siting of DGs in balanced radial distribution networks for loss minimization. International Journal of Electrical Power & Energy Systems, 67, 191-201. DOI: 10.1016/j.ijepes.2014.11.017

[11] Mahmoud, K., Yorino, N., & Ahmed, A. (2015). Optimal distributed generation allocation in distribution systems for loss minimization. IEEE Transactions on power systems, 31(2), 960-969. DOI: 10.1109/TPWRS.2015.2418333

[12] Kayal, P., Chanda, S., & Chanda, C. K. (2017). An analytical approach for allocation and sizing of distributed generations in radial distribution network. International Transactions on Electrical Energy Systems, 27(7), e2322. DOI: 10.1002/etep.2322

[13] El-Fergany, A. (2015). Optimal allocation of multi-type distributed generators using backtracking search optimization algorithm. International Journal of Electrical Power & Energy Systems, 64, 1197-1205. DOI: 10.1016/j.ijepes.2014.09.020

[14] Abou El-Ela, A. A., El-Sehiemy, R. A., & Abbas, A. S. (2018). Optimal placement and sizing of distributed generation and capacitor banks in distribution systems using water cycle algorithm. IEEE Systems Journal, 12(4), 3629-3636. DOI: 10.1109/JSYST.2018.2796847

[15] Pham, T. D., Nguyen, T. T., & Dinh, B. H. (2021). Find optimal capacity and location of distributed generation units in radial distribution networks by using enhanced coyote optimization algorithm. Neural Computing and Applications, 33(9), 4343-4371. DOI: 10.1007/s00521-020-05239-1

[16] Sultana, S., & Roy, P. K. (2014). Multi-objective quasi-oppositional teaching learning based optimization for optimal location of distributed generator in radial distribution systems. International Journal of Electrical Power & Energy Systems, 63, 534-545. DOI: 10.1016/j.ijepes.2014.06.031

[17] Nagaballi, S., & Kale, V. S. (2020). Pareto optimality and game theory approach for optimal deployment of DG in radial distribution system to improve techno-economic benefits. Applied Soft Computing, 92, 106234. DOI: 10.1016/j.asoc.2020.106234

[18] Sharma, S., Bhattacharjee, S., & Bhattacharya, A. (2016). Quasi-Oppositional Swine Influenza Model Based Optimization with Quarantine for optimal allocation of DG in radial distribution network. International Journal of Electrical Power & Energy Systems, 74, 348-373. DOI: 10.1016/j.ijepes.2015.07.034

[19] Imran, A. M., Kowsalya, M., & Kothari, D. P. (2014). A novel integration technique for optimal network reconfiguration and distributed generation placement in power distribution networks. International Journal of Electrical Power & Energy Systems, 63, 461-472. DOI: 10.1016/j.ijepes.2014.06.011

[20] Rao, R. S., Ravindra, K., Satish, K., & Narasimham, S. V. L. (2012). Power loss minimization in distribution system using network reconfiguration in the presence of distributed generation. IEEE transactions on power systems, 28(1), 317-325. DOI: 10.1109/TPWRS.2012.2197227

[21] Kowsalya, M. (2014). Optimal size and siting of multiple distributed generators in distribution system using bacterial foraging optimization. Swarm and Evolutionary computation, 15, 58-65. DOI: 10.1016/j.swevo.2013.12.001

[22] Balu, K., & Mukherjee, V. (2021). Optimal siting and sizing of distributed generation in radial distribution system using a novel student psychology-based optimization algorithm. Neural Computing and Applications, 33(22), 15639-15667. DOI: 10.1007/s00521-021-06185-2

[23] Khasanov, M., Kamel, S., Rahmann, C., Hasanien, H. M., & Al-Durra, A. (2021). Optimal distributed generation and battery energy storage units integration in distribution systems considering power generation uncertainty. IET Generation, Transmission & Distribution, 15(24), 3400-3422. DOI: 10.1049/gtd2.12230

[24] Uniyal, A., & Sarangi, S. (2021). Optimal network reconfiguration and DG allocation using adaptive modified whale optimization algorithm considering probabilistic load flow. Electric Power Systems Research, 192, 106909. DOI: 10.1016/j.epsr.2020.106909

[25] El-maksoud, A., Ahmed, A. H., & Hasan, S. (2023). Simultaneous Optimal Network Reconfiguration and Allocation of Four Different Distributed Generation Types in Radial Distribution Networks Using a Graph Theory-Based MPSO Algorithm. International Journal of Intelligent Engineering & Systems, 16(2). DOI: 10.22266/ijies2023.0430.24

[26] Ehsan, A., & Yang, Q. (2018). Optimal integration and planning of renewable distributed generation in the power distribution networks: A review of analytical techniques. Applied Energy, 210, 44-59. DOI: 10.1016/j.apenergy.2017.10.106

[27] Ameli, A., Bahrami, S., Khazaeli, F., & Haghifam, M. R. (2014). A multiobjective particle swarm optimization for sizing and placement of DGs from DG

owner's and distribution company's viewpoints. IEEE Transactions on power delivery, 29(4), 1831-1840. DOI: 10.1109/TPWRD.2014.2300845

[28] Pon Ragothama Priya, P., Baskar, S., Tamil Selvi, S., & Babulal, C. K. (2023). Optimal allocation of distributed generation using evolutionary multi-objective optimization. Journal of Electrical Engineering & Technology, 18(2), 869-886. DOI: 10.1007/s42835-022-01269-y

[29] Settoul, S., Chenni, R., Zellagui, M., & Nouri, H. (2021). Optimal integration of renewable distributed generation using the whale optimization algorithm for techno-economic analysis. Lecture Notes in Electrical Engineering, 682, 513-532. DOI: 10.1007/978-981-15-6403-1_35

[30] Selim, A., Kamel, S., Jurado, F., Lopes, J. A. P., & Matos, M. (2021). Optimal setting of PV and battery energy storage in radial distribution systems using multi-objective criteria with fuzzy logic decision-making. IET generation, transmission & distribution, 15(1), 135-148. DOI: 10.1049/gtd2.12019

[31] Adepoju, G. A., Salimon, S. A., Adebayo, I. G., & Adewuyi, O. B. (2024). Impact of DSTATCOM penetration level on technical benefits in radial distribution network. e-Prime-Advances in Electrical Engineering, Electronics and Energy, 7, 100413. DOI: 10.1016/j.prime.2023.100413

[32] Gao, H., Diao, R., Zhong, Y., Zeng, R., Wu, Q., & Jin, S. (2024). Optimal allocation of distributed generation in active distribution power network considering HELM-based stability index. International Journal of Electrical Power & Energy Systems, 155, 109508. DOI: 10.1016/j.ijepes.2023.109508

[33] Adetunji, K. E., Hofsajer, I. W., Abu-Mahfouz, A. M., & Cheng, L. (2020). A review of metaheuristic techniques for optimal integration of electrical units in distribution networks. IEEE Access, 9, 5046-5068. DOI: 10.1109/ACCESS.2020.3048438

[34] Belbachir, N., Kamel, S., Hashim, F. A., Yu, J., Zeinoddini-Meymand, H., & Sabbeh, S. F. (2023). Optimizing the hybrid PVDG and DSTATCOM integration in electrical distribution systems based on a modified homonuclear molecules optimization algorithm. IET Renewable Power Generation, 17(12), 3075-3096. DOI: 10.1049/rpg2.12826

[35] Abdollahzadeh, B., Gharehchopogh, F. S., Khodadadi, N., & Mirjalili, S. (2022). Mountain gazelle optimizer: a new nature-inspired metaheuristic algorithm for global optimization problems. Advances in Engineering Software, 174, 103282. DOI: 10.1016/j.advengsoft.2022.103282

[36] Abdelsattar, M., Mesalam, A., Fawzi, A., & Hamdan, I. (2024). Mountain gazelle optimizer for standalone hybrid power system design incorporating a type of incentive-based strategies. Neural Computing and Applications, 36(12), 6839-6853. DOI: 10.1007/s00521-024-09433-3

[37] Mohammadzadeh, A., & Mirjalili, S. (2024). Eel and grouper optimizer: a nature-inspired optimization algorithm. Cluster Computing, 1-42. DOI: 10.1007/s10586-024-04545-w

[38] Kyrou, G., Charilogis, V., & Tsoulos, I. G. (2024). Refining the Eel and Grouper Optimizer with Intelligent Modifications for Global Optimization. Computation, 12(10). DOI: 10.3390/computation12100205

[39] Aman, M. M., Jasmon, G. B., Bakar, A. H. A., & Mokhlis, H. (2014). A new approach for optimum simultaneous multi-DG distributed generation Units placement and sizing based on maximization of system loadability using HPSO (hybrid particle swarm optimization) algorithm. Energy, 66, 202-215. DOI: 10.1016/j.energy.2013.12.037